Dendrimeric Liquid Crystals: Isotropic−Nematic Pretransitional Behavior

Jian-feng Li,[†] Karl A. Crandall,[†] Peihwei Chu,[‡] Virgil Percec,[‡] Rolfe G. Petschek,[†] and Charles Rosenblatt*[,†,‡]

Departments of Physics and Macromolecular Science, Case Western Reserve University, Cleveland, Ohio 44106

Received July 26, 1996; Revised Manuscript Received September 11, 1996[⊗]

ABSTRACT: Kerr measurements, ellipsometry, and quasielastic light scattering have been used to probe nematic fluctuations and nematic wetting at an isotropic liquid crystal−substrate interface in four generations of liquid crystalline monodendrons and dendrimers. We find that the pretransitional behavior is qualitatively similar to that of low molecular weight liquid crystals, exhibiting a Landau-like divergence of the relaxation time and a logarithmic divergence of the optical retardation on approaching the nematic−isotropic phase transition from above. Quantitatively, we find that the transition temperatures of the monodendrons are typically about 0.5 K above the supercooling limit of the isotropic phase and that the orientational viscosities may be fit to a power law in molecular weight M_n, where the exponent ≤ 1.0.

Introduction

Dendrimers and hyperbranched polymers are macromolecular compounds which contain a branching point in each structural repeat unit.[1−5] The shape of the three-dimensional architecture resulting from these novel polymers can range from ellipsoidal to cylindrical and spherical, where this complex structural capability presents numerous possibilities for new material properties. Recent publications from one of our laboratories reported the first examples of hyperbranched polymers exhibiting thermotropic calamitic[6] and columnar hexagonal[7] liquid crystalline phases. Hyperbranched polymers exhibiting lyotropic[8] and thermotropic[9] liquid crystalline phases have since been synthesized in other laboratories. Recently, we reported the first examples of monodendrons and dendrimers which display thermotropic cybotactic nematic and smectic phases.[10] The goal of this publication is to report on a series of optical measurements in the isotropic phase above the nematic transition on the first four generations of monodendrons G_n(OH) and dendrimers $G_n(D_3)$, where $n = 1-4$ represents the generation number. Kerr and dynamic light scattering measurements in the isotropic phase show that the orientational relaxation time τ *vs* temperature is qualitatively consistent with a Landau−de Gennes mean field model, typical of most low molecular weight liquid crystals. Quantitatively, however, we find that τ for the dendrimer $G_n(D_3)$ is only about twice that of the monodendron G_n(OH) for the corresponding generation n. [The molecular weight of the dendrimer is more than 3 times that of the monodendron.] Additionally, the adsorption parameter Γ, corresponding to the integrated birefringence, *i.e.*, $\Gamma \equiv \int k\Delta n \, dz$ (ref 11), was measured for the monodendron in the isotropic phase by ellipsometry. The results indicate that the surface-induced orientational order parameter is larger than the discontinuity δS of the bulk order parameter at the nematic−isotropic phase transition and that the nematic phase completely wets the interface.

Experimental Section

The structures of the monodenrons and dendrimers, together with their molecular weights, are illustrated in Charts 1 and 2. In these structures the mesogenic repeat unit is in its *gauche* conformation as it most probably exists in solution. X-ray diffraction experiments performed in the cybotactic nematic, smectic, and crystalline phases have shown that in all these phases the mesogenic repeat units are in their *anti* conformation. Scheme 1 shows the interconversion from the *anti* to the *gauche* conformation and the overall shape of the monodendron in the nematic phase. The synthesis of the monodendrons and dendrimers is discussed in refs 10 and 12.

Relaxation time measurements were made using an electrically induced birefringence scheme, *i.e.*, the Kerr technique. Two glass slides coated with indium tin oxide (ITO) were separated by mylar spacers of nominal thickness 6 μm. The cell was filled with the appropriate dendrimer in the isotropic phase and was placed into an oven which was temperature controlled to 10 mK. The beam from a 5 mW He−Ne laser was directed along the $\hat{z}$-axis and passed consecutively through a polarizer oriented at 45° with respect to the $\hat{x}$-axis, a Babinet−Soleil compensator, the sample, a crossed analyzer, and into a photodiode detector. The compensator was adjusted so that, in the absence of an applied voltage to the sample, the optical retardation $\alpha_{comp} = \pi/4$. In order to detect the electrically induced optical phase shift α_{sample} through the sample, the cell was tilted by an angle $\varphi = 45°$ in the $\hat{x}-\hat{z}$ plane, thereby making the $\hat{x}$-axis the extraordinary optical axis. The resulting detector output was input to a two-phase lock-in amplifier which was reference to the ac voltage applied to the sample; in this configuration the lock-in signal was proportional to α_{sample}, which in turn was proportional to the field-induced orientational order parameter S. An ac voltage of amplitude 30 V rms and frequency $\omega = 1992$ s^{-1} (corresponding to 317 Hz) was applied to the sample, and both the in-phase and 90° out-of-phase (quadrature) components of the signal were measured by the lock-in amplifier at 2ω. It can be shown[13] that, for a free energy density of the form

$$F \equiv F_N + {}^1/_2L(\nabla S)^2 - {}^1/_3\Delta\chi E^2 S = {}^1/_2a(T - T^*)S^2 - {}^1/_3bS^3 + {}^1/_4cS^4 + {}^1/_2L(\nabla S)^2 - {}^1/_3\Delta\chi E^2 S \quad (1)$$

the component of induced order $S_{2\omega}$ at frequency 2ω is given by

$$S_{2\omega} = \frac{\Delta\chi E_0{}^2}{6a(T - T^*)[1 + 4\omega^2\tau^2]}(\cos 2\omega t + 2\omega\tau \sin 2\omega t) \quad (2)$$

where a, b, c, and L are constants, T^* is the supercooling limit of the isotropic phase, $\Delta\chi$ is the electric susceptibility anisotropy, and $E = E_0 \cos \omega t$. The correlation length ξ for

* To whom correspondence should be addressed.
† Department of Physics.
‡ Department of Macromolecular Science.
⊗ Abstract published in *Advance ACS Abstracts,* November 1, 1996.

S0024-9297(96)01116-3 CCC: $12.00

Chart 1. Structures and Molecular Weights of G_n(OH) Monodendrons ($n = 1-4$)

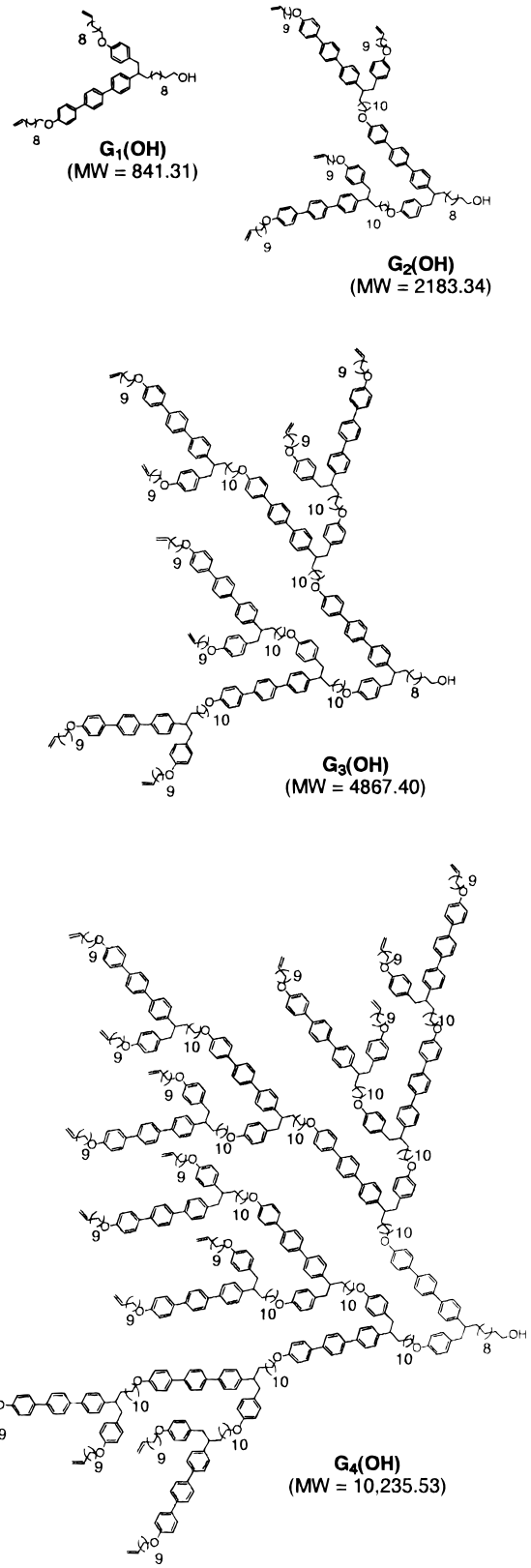

orientational fluctuations is $\xi \equiv \{L/[a(T - T^*)]\}^{1/2}$, and the relaxation time τ is[13]

$$\tau = \frac{\eta}{a(T - T^*)} = \frac{S_{2\omega}^{\text{quad}}}{2\omega S_{2\omega}^{\text{in-phase}}} \qquad (3)$$

where η is the viscosity. The relaxation time *vs* temperature was obtained according to eq 3, and its inverse τ^{-1} is shown in Figure 1 for the monodendrons and in Figure 2 for the dendrimers. Numerical data are presented in Table 1.

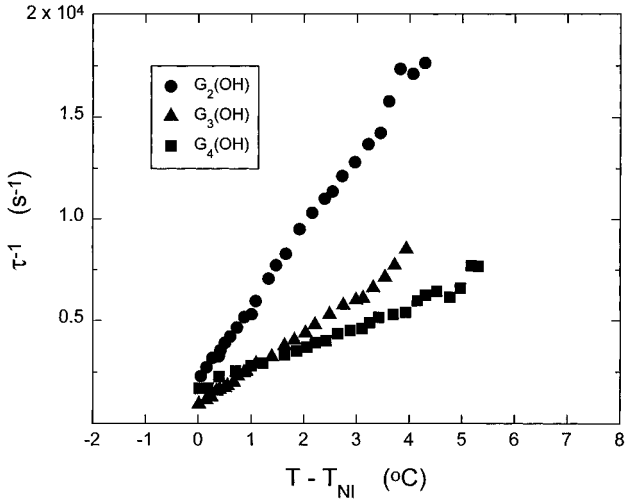

Figure 1. Inverse relaxation time τ^{-1} *vs* $T - T_{NI}$ obtained from Kerr measurements for the three monodendrons G_n(OH) ($n = 2-4$).

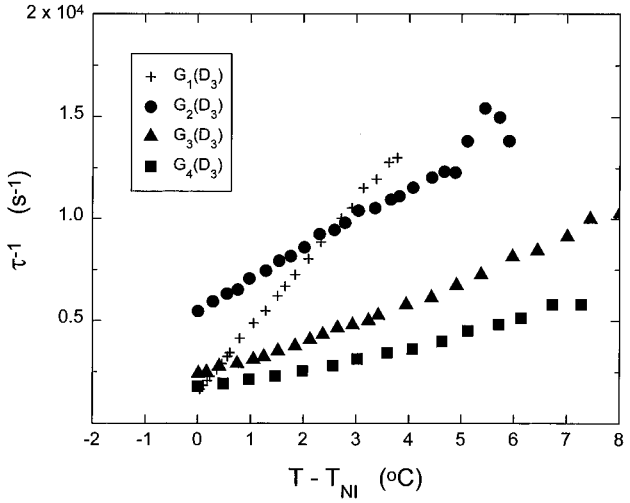

Figure 2. Inverse relaxation time τ^{-1} *vs* $T - T_{NI}$ obtained from Kerr measurements for the four dendrimers $G_n(D_3)$ ($n = 1-4$).

An estimate of the correlation length, as well as a consistency check of the Kerr results, was made by performing a depolarized light scattering measurement on G_2(OH). A rectangular glass cuvette of optical path length 1 cm was filled with approximately 0.5 g of G_2(OH) and placed into an oven, which was temperature controlled to approximately 50 mK. Light from an Ar ion laser operating at wavelength $\lambda = 5145$ Å was normally incident on one face of the cuvette, with polarization normal to the scattering plane. The scattered light was detected at 90° by a photomultiplier tube (PMT) detector, having first passed through a polarizer whose axis was in the scattering plane. This geometry corresponds to a homodyne VH depolarized scattering measurement with wavevector $q = 2.72 \times 10^5$ cm^{-1} for refractive index $n = 1.573$ just above T_{NI}. The output from the PMT passed through a pulse amplifier−discriminator and into a Brookhaven Instruments Model BI-2030AT digital autocorrelator. The entire apparatus is described in detail elsewhere.[14] At each temperature in the isotropic phase an autocorrelation function was obtained, whose single-exponential decay was appropriate for correlated orientational fluctuations. The amplitude and decay time τ were obtained from a two-parameter least-squares fit to the data—the baseline of the exponential was obtained experimentally from the average of six delay channels—and τ^{-1} is plotted in Figure 3 *vs* temperature.

Chart 2. Structures and Molecular Weights of $G_n(D_3)$ Dendrimers ($n = 1-4$)

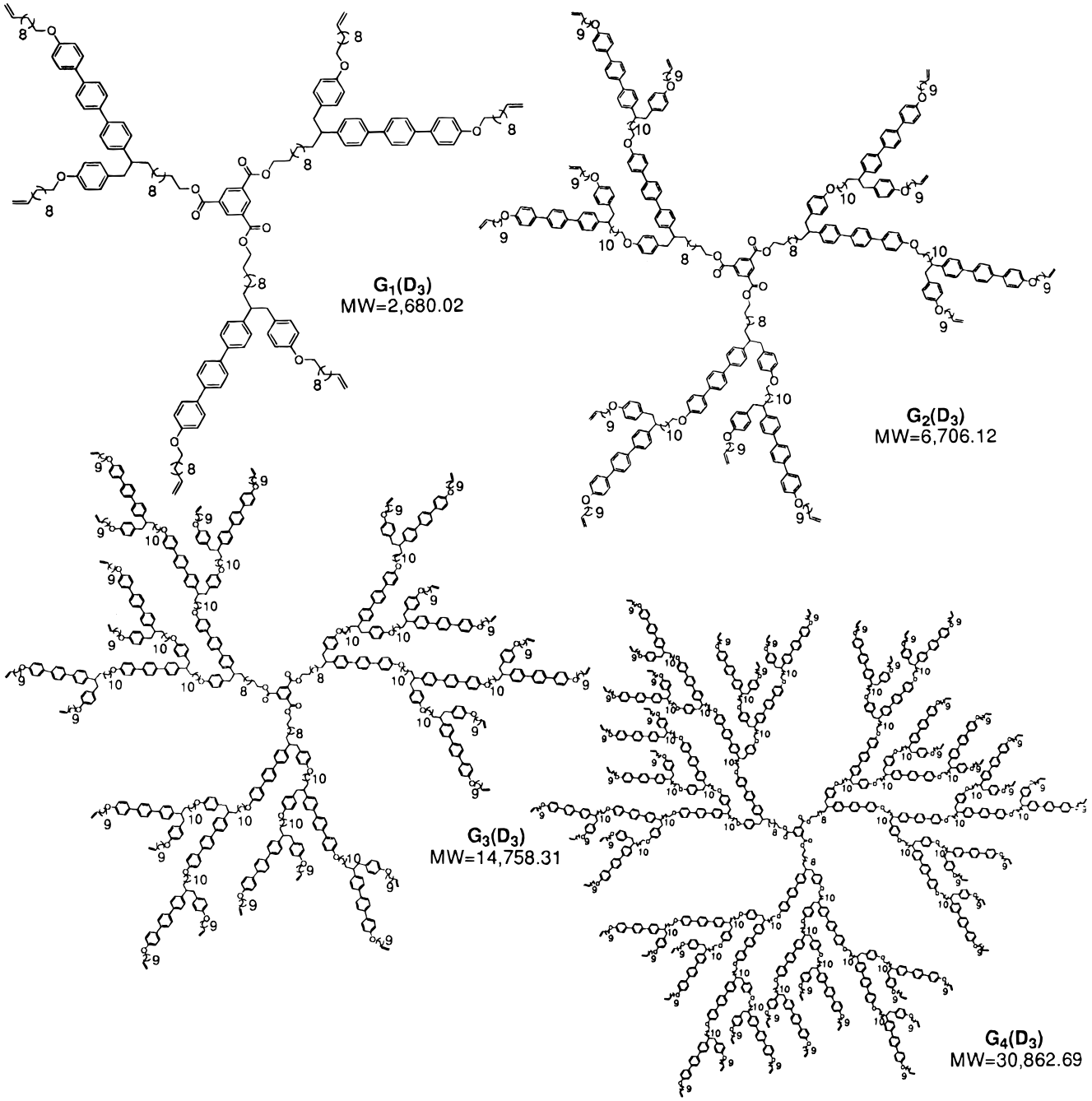

To examine pretransitional wetting of the surface by the nematic phase, two glass substrates were dipped in a 1% w/w mixture of nylon 6/6 in formic acid and allowed to air-dry. The surfaces were then rubbed unidirectionally on paper to promote planar alignment. The glass slides were then placed together, separated by mylar spacers of nominal thickness 3 μm, and epoxied along two edges. Three such cells were constructed, and each cell was filled in the isotropic phase with one of the monodendrons G_n(OH). On cooling into the nematic phase, good planar alignment was observed under a polarizing microscope. We should note that a two-phase region was apparent around the NI transition for each sample, such that the extent of the two-phase region had an upper bound of ~50 mK. The G_n(OH) cells were then reheated into the isotropic phase in an oven designed for optical ellipsometry, where the temperature was controlled to 25 mK. The entire oven was placed into a birefringence apparatus based upon a modulated Pockels cell which is described in detail elsewhere,[15] and the optical retardation $\Gamma \equiv \int k\Delta n \, dz$ was recorded as a function of temperature. Data were taken approximately every 3 min, permitting sufficient time for the temperature to stabilize between measurements. Figures 4–6 show the retardation *vs* temperature results for G_2(OH), G_3(OH), and G_4(OH), respectively; the monomer data is not shown, as it was flat down to T_{NI}, showing no discernible pretransitional behavior in the isotropic phase.

Results and Discussion

On approaching the nematic–isotropic phase transition from above, one finds a pretransitional increase in the nematic susceptibility. Both the susceptibility and the relaxation time diverge toward a supercooling temperature T^* before being cut off by the first-order phase transition at T_{NI}. The data in Figures 1 and 2 are consistent with this model, as seen by the linearity of τ^{-1} *vs* temperature, and are qualitatively analogous to low molecular weight data for, *e.g.*, methoxybenzylidenebutylaniline (MBBA).[16] Quantitatively, however, differences exist between the low molecular weight liquid crystal data and that of the dendrimers. Perhaps

Table 1

material	M_n[a]	$[\eta/a] \times 10^4$ (s °C)	transition Temp T_{NI} (°C)	supercooling limit T^* (°C)
G_2(OH)	3540	2.6 ± 0.1	93.3	92.9
G_3(OH)	7200	5.6 ± 0.2	105.5	105.0
G_4(OH)	14308	9.5 ± 0.3	111.5	110.1
$G_1(D_3)$	3588	3.2 ± 0.1	74.5	74.0
$G_2(D_3)$	8679	6.4 ± 0.2	100.5	97.0
$G_3(D_3)$	17607	10.3 ± 0.4	107.3	105.2
$G_4(D_3)$	33118	17.2 ± 0.5	110.7	108.4

[a] Molecular weight data after ref 10. Molecular weight distributions are $M_w/M_n \leq 1.09$.

most obvious is that, owing largely to their higher viscosities, the relaxation times for the dendrimers are about 2 orders of magnitude slower than that of MBBA at comparable $T - T^*$. We also note that for a given class of monodendrons G_n(OH) and dendrimers $G_n(D_3)$, the quantity η/a (*cf.* eq 3) increases with increasing molecular weight M_n (Figure 7). We may fit the ratio η/a to a power law, *viz.*, $\eta/a \propto M_n^x$. For the monodendrons we obtain $x = (0.85 \pm 0.15)$ and for the dendrimers $x = (0.75 \pm 0.03)$. In a rheometric measurement of the shear viscosity in the melt phase, Hawker *et al.* found an evolution in the viscosity exponent with molecular weight,[17] approaching the disentangled Rouse prediction $x = 1$ for molecular weights $> 10^4$. Moreover, their data showed no sharp transition which might be associated with the onset of entanglement, nor did their data show a large quantitative difference in viscosities between the monodendrons and dendrimers. We observed similar, although not identical, behavior in our measurements in the isotropic phase. To be sure, our measurements in the isotropic phase correspond to the ratio η/a, where η is an *orientational viscosity* associated with the onset of nematic order, whereas ref 17 describes a bulk shear viscosity. If we assume that the Landau coefficient a is independent of generation number, then our exponents x would correspond to the variation of the orientational viscosity with M_n. To lowest order the constant a approximation is equivalent to untethering the mesogens. The constant a approximation may not be completely valid, however. For example, one may still need to account for the variation of a with the ratio R of spacer groups to mesogenic groups. In main-chain oligomers it has been shown that the coefficient a increases with R,[18] which would have the effect of slightly increasing the effective exponents for the *absolute* viscosity η relative to the exponents for the *ratio* η/a.

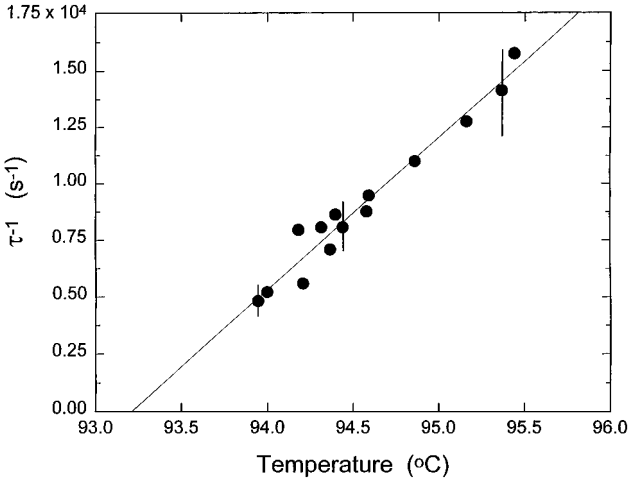

Figure 3. Inverse relaxation time τ^{-1} *vs* temperature obtained from light scattering measurements at $q = 2.72 \times 10^5$ cm^{-1} for G_2(OH). Solid line represents a linear least-squares fit. The intersection of the fitted line with the abscissa corresponds to the supercooling limit T^* of the isotropic phase. Typical error bars are shown.

Scheme 1. Dynamic Equilibrium between the Structures of G_2(OH) Resulting from *gauche* and *anti* Conformers and Their Structural Repeat Units with the Structure of G_2(OH), G_3(OH), and G_4(OH) Obtained with Their Structural Units in the *anti* Conformation

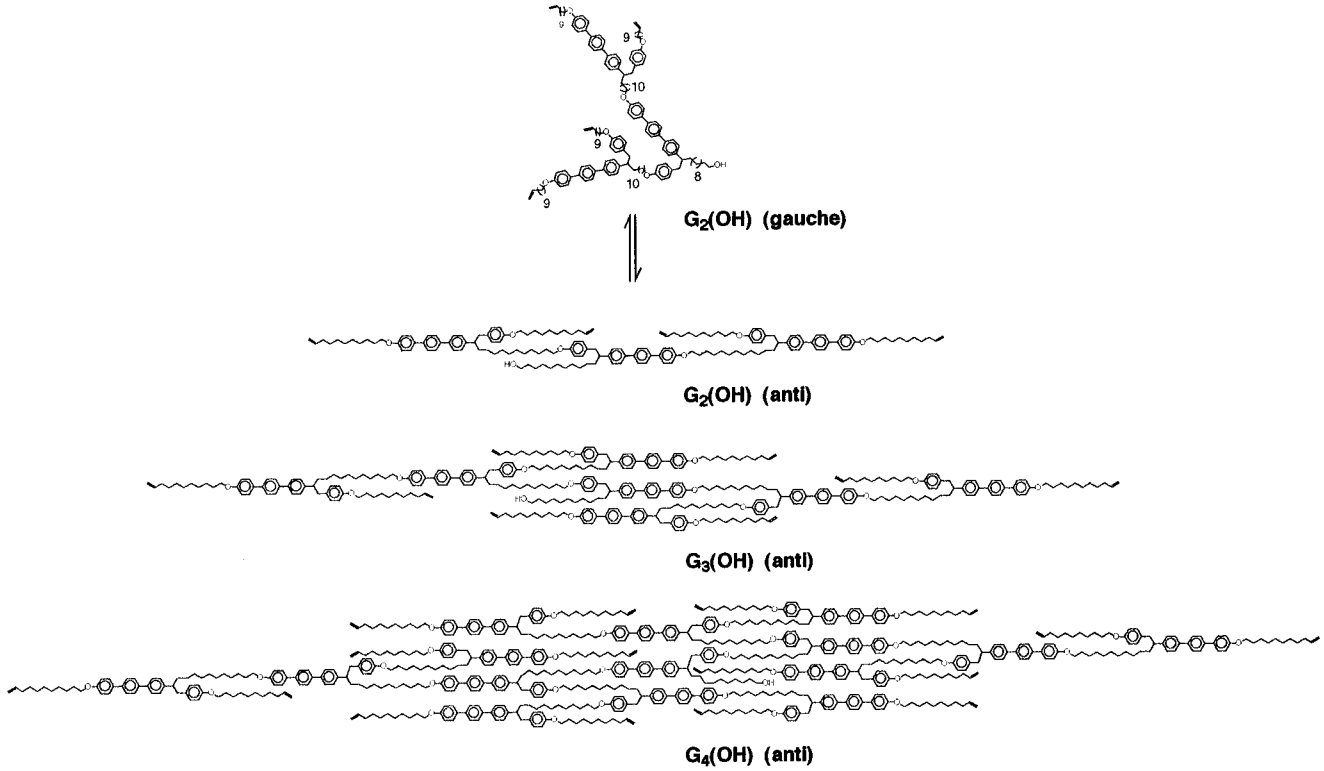

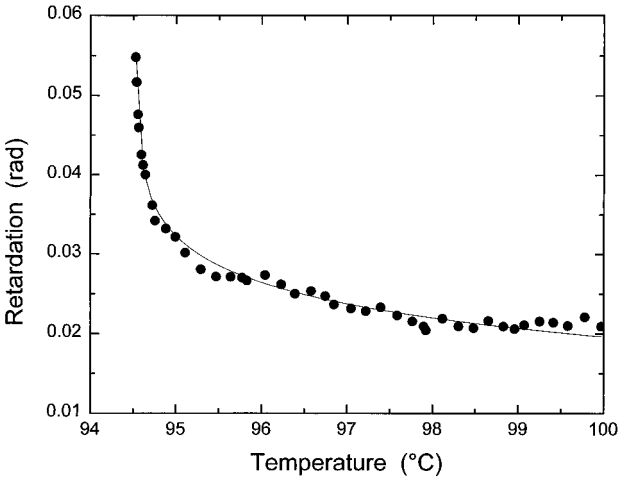

Figure 4. Optical retardation α_{sample} *vs* temperature for G_2-(OH). Solid line represents a least-squares fit to eq 5.

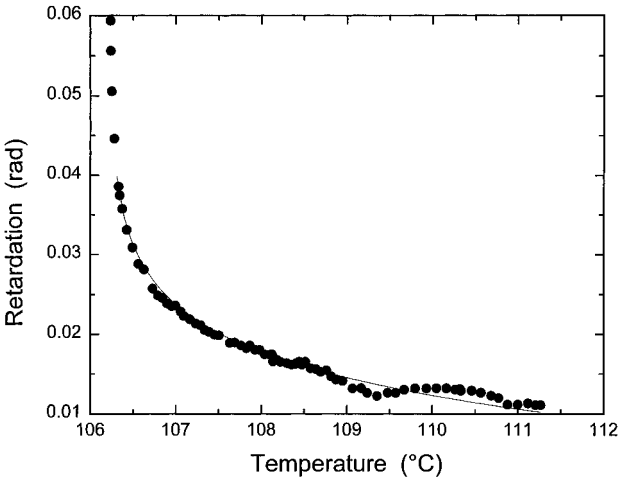

Figure 5. Same as for Figure 4, except for G_3(OH).

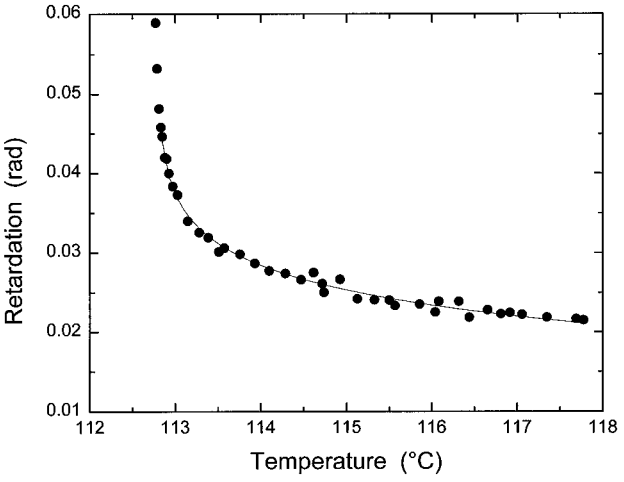

Figure 6. Same as for Figure 4, except for G_4(OH).

It is interesting to note that in our measurements both monodendrons and dendrimers have similar values of η/a *vs* M_n. Additionally, the orientational viscosity of our monodendrons exhibits concave downward behavior on a log−log plot, indicating an *evolution* of x with M_n. Clearly, our exponential fit with $x = (0.85 \pm 0.15)$ for the monodendrons was inappropriate. The monodendron exponent asymptotically approaches $x \approx 0.75$ at large M_n, comparable to the exponent for the dendrimer, and slightly smaller than those of ref 17. (As noted above, a variation of the coefficient a with M_n might have the effect of slightly increasing the exponent for η alone.) Additionally, like ref 17, our data show no apparent jump in viscosity. With the caveat that we have used a limited number of data points for the two fits, we might infer that the dynamics of orientational ordering are coupled strongly to the motion of the dendrimer, and thus our measured exponents would be similar to, but slightly smaller smaller than, the shear viscosity exponents of ref 17. This is indeed the case. Moreover, given the relatively small exponents ($|x| \lesssim 1$), it is likely that the dendrimers are not entangled. The higher symmetry of the dendrimer may be responsible for the smaller exponent, as its motion is less impeded than that of the monodendron.

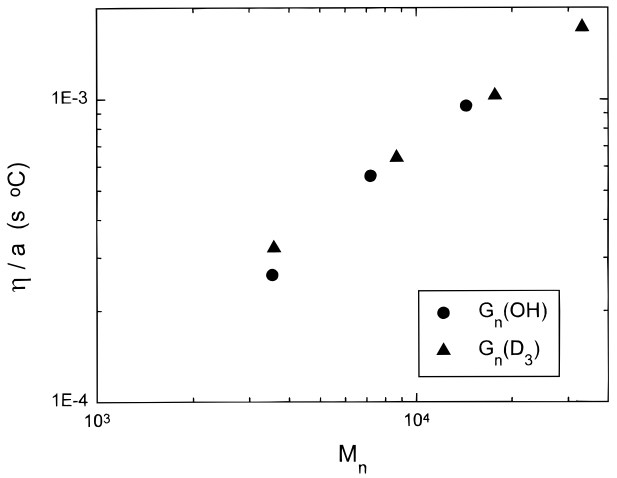

Figure 7. η/a *vs* M_n for monodendrons (●) and dendrimers (▲).

A more subtle result is the quantity $T_{NI} - T^*$, the temperature difference between the first-order phase transition and the supercooling limit. For MBBA—indeed, for most low molecular weight liquid crystals—this quantity is of order 2 K, as it is also for the dendrimers $G_n(D_3)$. For the monodendrons G_n(OH), however, the quantity $T_{NI} - T^*$ is approximately 0.5 K, as can be seen from Table 1. In earlier work on the cyclic trimer TPB-(c)9(3) Li *et al.* found $T_{NI} - T^*$ to be less than 200 mK.[13] A small value of $T_{NI} - T^*$ is often associated with a nearby Landau point on a temperature−molecular architecture phase diagram, such that the isotropic phase and a biaxial and two uniaxial nematic phases coexist at this point.[19−22] Moreover, the transition from the isotropic phase into the nematic is continuous at the Landau point, corresponding to the coefficient $b \rightarrow 0$ in eq 1. Thus, if the transition from isotropic to a uniaxial nematic phase is near the Landau point, in general one would expect a reduction in the quantity $T_{NI} - T^*$, as well as significant biaxial character. Indeed, TPB-(c)9(3) exhibits behavior consistent with a uniaxial−biaxial nematic phase transition at ∼30 °C below T_{NI}, compatible with a nearby Landau point.[23] Because of the relatively small value of $T_{NI} - T^*$ for the monodendrons G_n(OH), one might therefore expect to find a significant biaxial character in these materials in the form of large biaxial nematic fluctuations within the uniaxial phase. On the other hand, the larger value of $T_{NI} - T^*$ for the dendrimers is consistent with the higher symmetry of its molecular shape. Detailed investigations of biaxiality are beyond the scope of the present work, but will be considered in the future. Another result apparent from Figures 1 and 2 is that the relaxation times for the dendrimers $G_n(D_3)$ are only about twice as long as those of the monodendrons

G_n(OH), although their molecular weights are only one-third those of the dendrimers. This behavior was first noted qualitatively by Percec *et al.*,[10] where it was observed that the magnetically induced director reorientational times of the dendrimers in the nematic phase are comparable to their monodendron counterparts. This is a somewhat surprising result, and indicates that the mesogenic moieties orient relatively freely.

Turning now to the light scattering results of Figure 3, we note that the VH scattering geometry probes a single relaxation time $\tau = \eta/[a(T - T^*)(1 + \xi^2 q^2)]$. For low molecular weight materials, we typically find $\xi^2 q^2 < 0.1$ at the NI transition (where $\xi \sim 100-150$ Å), even for 90° scattering. We would therefore expect that τ from the light scattering results would be comparable to the Kerr results (*cf.* eq 3). Clearly, the scattering results in Figure 3 exhibit the desired mean field behavior; *viz.*, τ^{-1} is linear in $T_{NI} - T^*$. However, near the first-order phase transition temperature the relaxation rates τ^{-1} for G_2(OH) as measured by light scattering are about twice as fast as those measured by the Kerr technique. To understand this behavior, we note that if the correlation length near T_{NI} were large, the relaxation times, which scale as $(1 + \xi^2 q^2)^{-1}$, would be reduced accordingly. For our scattering wavevector $q = 2.72 \times 10^5$ cm^{-1}, a correlation length of $\xi \sim 350$ Å would be required to reduce τ by approximately one-half relative to the (zero wavevector) Kerr measurement, as indicated by the data. Is this relatively large correlation length surprising? Probably not, because the correlation length ξ diverges as $\xi_0(T_{NI} - T^*)^{-1}$ in mean field theory and $T_{NI} - T^*$ for G_2(OH) is approximately one-third the value typically found in low molecular weight liquid crystals.[16] Here ξ_0 is the "bare" correlation length. In this light we would conclude that the bare correlation length for the monodendron is similar to that of low molecular weight liquid crystals.

We now turn our attention to the birefringence data. Miyano *et al.* first examined the pretransitional rise in Γ on approaching the NI phase transition from above[24-26] and discussed their results in terms of surface-induced orientational order propagating into the bulk. Expanding on these ideas, the Berkeley group developed an evanescent wave technique to facilitate the separate extraction of the surface orientational order parameter S_s and the correlation length associated with the growth of the nematic region at the interface.[27,28] The theory behind the growth of a nematic layer at the interface has been addressed by several groups,[29-31] generally adopting a mean field approach using either a specific potential or a general Landau expansion. Perhaps the simplest tack involves neglecting biaxiality, integrating the Euler−Lagrange equation obtained from the free energy eq 1 and imposing a boundary condition S_s at the surface. In practice, S_s may be a (generally) weak function of temperature,[24] although such a dependence considerably complicates the analysis. After considerable manipulation, one finds that Γ may be written[25] in the form $\Gamma = \text{const} \times \ln[P(T,S_s)]$, where const depends upon the Landau coefficients L and c and the saturated birefringence of the liquid crystal, and

$$P(T,S_s) = \frac{[F_N(S_s)]^{1/2} + [{}^1/_2 a(T - T^*)]^{1/2} + {}^1/_2 S_s c^{1/2}}{[F_N(S_s)]^{1/2} + [{}^1/_2 a(T - T^*)]^{1/2} - {}^1/_2 S_s c^{1/2}} \quad (4)$$

Here $F_N(S)$ is the free energy density of the spatially uniform nematic phase in the absence of an electric field (*cf.* eq 1). For $S_s < \delta S$, we find that Γ exhibits a cusp at T_{NI}; for $S_s > \delta S$, however, Γ exhibits a (slow) logarithmic divergence at T_{NI}. In this case, Γ has the asymptotic form[27]

$$\Gamma = -c_1 \ln\left(\frac{T - T_{NI}}{T_{NI}}\right) + c_2 \quad (5)$$

where the constants c_1 and c_2 depend on the bulk Landau coefficients for the particular material, and c_2 depends upon S_s. For materials for which the Landau coefficients are well known, it is possible to extract the order parameter S_s at the surface.[27] For the dendrimers, however, these coefficients have not yet been determined. Nevertheless, we see from Figures 4−6 that the data may be well fitted by eq 5 if we assume a temperature-independent S_s. This would indicate that the order parameter induced by the surface S_s is seemingly larger than the discontinuity δS of the bulk nematic order parameter at the NI phase transition, with the possible exception of G_3(OH) at its rubbed surface (Figure 5). The apparent differences in offsets are due to the not very good reproducibility of the rubbed nylon surface from sample to sample. In fact, depending upon the quality of the buffing, the surface order parameter S_s could be smaller than the bulk order parameter discontinuity δS, and a cusp at T_{NI} would obtain. This *may* be the case for G_3(OH), although the data are equivocal for this material. Additionally, we should note that some experimental uncertainty exists—approximately ±0.05 rad—in the offset due to alignment of the Pockels cell. This would have the main effect of shifting c_2 up or down by a temperature-independent constant and thus introduce some uncertainty into the determination of S_s. Nevertheless, the main feature of Figures 4−6 remains the slow logarithmic divergence of the retardation toward T_{NI}, a feature similar to that which may be associated with low molecular weight liquid crystals and surface treatments which induce a large degree of orientational order at the interface.

Summary

From the foregoing discussion we see that in several respects the NI transition associated with dendrimer liquid crystals may be quite similar to the analogous transition in low molecular weight materials. Both classes of materials exhibit Landau-like mean field behavior in the isotropic phase, nematic fluctuations. The monodendrons G_n(OH) may also exhibit incipient biaxial character to a greater extent than the dendrimers and rodlike low molecular weight materials. Light scattering results suggest a larger correlation length at the NI transition for the monodendron G_2(OH), which is due to its much closer approach to the supercooling limit T^* than typical crystalline molecules. The monodendrons, as do low molecular weight liquid crystals, may exhibit substantial wall-induced orientational order, which gives rise to a logarithmic divergence in the retardation on approaching T_{NI}. The similarities may extend into the nematic phase as well, although one might expect to see very different elastic constants in the dendrimers as compared to the low molecular weight materials. These investigations are now underway. Clearly, dendrimer liquid crystals are an interesting alternative for better understanding existing phenomena, and offer the prospect of different and potentially exotic new phenomena in the lower temperature phases.

Acknowledgment. We are indebted to Profs. Alexander Jamieson and Shi-Qing Wang for important discussions. This work was supported by the National Science Foundation under Grant DMR-9122227.

References and Notes

(1) Tomalia, D. A. *Sci. Am.* **1995**, May, 62.
(2) Ardoin, N.; Astruc, D. *Bull. Soc. Chim. Fr.* **1995**, 875.
(3) Fréchet, J. M. J. *Science* **1994**, *263*, 1710.
(4) Tomalia, D. A.; Durst, H. D. *Top. Curr. Chem.* **1993**, *165*, 193.
(5) Vögtle, F.; Issberner, J.; Moors, R. *Angew. Chem., Int. Ed. Engl.* **1994**, *33*, 2413.
(6) Percec, V.; Kawasume, M. *Macromolecules* **1992**, *25*, 3843.
(7) Percec, V.; Cho, C. G.; Pugh, C.; Tomazos, D. *Macromolecules* **1992**, *25*, 1164.
(8) Kim, Y. H. *J. Am. Chem. Soc.* **1992**, *114*, 4947.
(9) Bauer, S.; Fischer, H.; Ringsdorf, H. *Angew. Chem., Int. Ed. Engl.* **1993**, *25*, 1589.
(10) For a highlight, see: Percec, V.; Chu, P.; Ungar, G.; Zhou, J. *J. Am. Chem. Soc.* **1995**, *117*, 11441.
(11) Miyano, K. *J. Chem. Phys.* **1979**, *71*, 4108.
(12) Percec, V.; Chu, P. *Polym. Prepr. (Am. Chem. Soc., Div. Polym. Chem.)* **1995**, *36*, 743.
(13) Li, J.-F.; Percec, V.; Rosenblatt, C. *Phys. Chem. Rev. E* **1993**, *48*, R1.
(14) DiLisi, G. A.; Rosenblatt, C.; Griffin, A. C.; Hari, U. *Phys. Rev. A* **1992**, *45*, 5738.
(15) Rosenblatt, C. *J. Phys. (Paris)* **1984**, *45*, 1087.
(16) Stinson, T. W.; Litster, J. D.; Clark, N. A. *J. Phys. (Paris) Colloq.* **1972**, *33*, C1−69.
(17) Hawker, C. J.; Farrington, P. J.; Mackay, M. E.; Wooley, K. L.; Fréchet, J. M. J. *J. Am. Chem. Soc.* **1995**, *117*, 4409.
(18) Rosenblatt, C.; Griffin, A. C. *Macromolecules* **1989**, *22*, 4102.
(19) Priest, R. G.; Lubensky, T. C. *Phys. Rev. B* **1976**, *13*, 4159.
(20) Alben, R. *Phys. Rev. Lett.* **1973**, *30*, 778.
(21) Shih, C. S.; Alben, R. *J. Chem. Phys.* **1972**, *57*, 3055.
(22) Melnik, G.; Photinos, P.; Saupe, A. *J. Chem. Phys.* **1988**, *88*, 4046.
(23) Li, J.-F.; Percec, V.; Rosenblatt, C.; Lavrentovich, O. D. *Europhys. Lett.* **1994**, *25*, 199.
(24) Miyano, K. *J. Chem. Phys.* **1979**, *71*, 4108.
(25) Tarczon, J. C.; Miyano, K. *J. Chem. Phys.* **1980**, *73*, 1994.
(26) Miyano, K. *Phys. Rev. Lett.* **1979**, *43*, 51.
(27) Chen, W.; Martinez-Miranda, L. J.; Hsiung, H.; Shen, Y. R. *Phys. Rev. Lett.* **1989**, *62*, 1860.
(28) Hsiung, H.; Rasing, Th.; Shen, Y. R. *Phys. Rev. Lett.* **1986**, *57*, 3065.
(29) Sheng, P. *Phys. Rev. Lett.* **1976**, *37*, 1059; *Phys. Rev. A* **1982**, *26*, 1610.
(30) Poniewierski, A.; Sluckin, T. J. *Liq. Cryst.* **1987**, *2*, 281.
(31) Allender, D. W.; Henderson, G. L.; Johnson, D. L. *Phys. Rev. A* **1981**, *24*, 1086.

MA961116B